analytical chemistry

Article

pubs.acs.org/ac

Non-Peptide-Based Fluorogenic Small-Molecule Probe for Elastase

Qi Sun,[†,§] Jun Li,[†,§] Wan-Nian Liu,[†] Qing-Jian Dong,[†] Wen-Chao Yang,*[,†] and Guang-Fu Yang*[,†,‡]

[†]Key Laboratory of Pesticide & Chemical Biology of Ministry of Education, College of Chemistry, Central China Normal University, Wuhan 430079, People's Republic of China

[‡]Collaborative Innovation Center of Chemical Science and Engineering, Tianjin 30071, People's Republic of China

Supporting Information

ABSTRACT: Human neutrophil elastase (HNE) has been identified as a potential therapeutic target for the discovery of anti-inflammatory drugs for decades. However, little progress has been made on assays measuring the activity of HNE, especially on synthetic substrates which play essential role in determination of HNE activity. Herein, a small-molecule compound, 2,2,3,3,3-pentafluoro-*N*-(2-oxo-4-(trifluoromethyl)-2*H*-chromen-7-yl)-propanamide (compound **4**), has been successfully designed as the first ever non-peptide-based fluorogenic substrate for HNE. A "turn-on" fluorometric assay based on **4** has been successfully developed for rapid determination of HNE activity and the inhibitory kinetic study. Most importantly, the probe **4** shows highly specific response for HNE among seven tested hydrolases or proteins and can be directly used to detect the elevated HNE activity in the serum of chronic obstructive pulmonary disease (COPD) patients compared to that of healthy controls. This specific and cost-effective probe will facilitate future high-throughput discovery of HNE inhibitors and clinical diagnosis of elastase-related diseases.

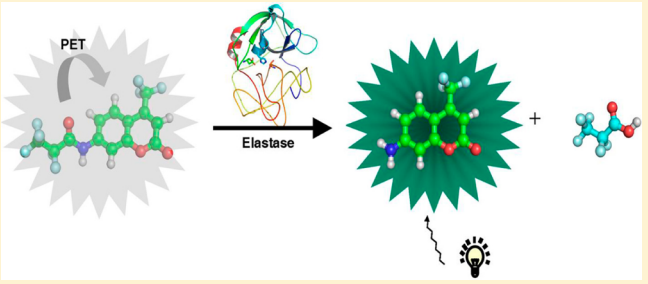

Human neutrophil elastase (HNE, EC 3.4.21.37), a 29 kDa serine protease, plays an important role in degrading proteins within both azurophil granules (specialized neutrophil lysosomes) and the extracellular matrix. HNE has been identified as a potential therapeutic target for the discovery of anti-inflammatory drugs,[1−3] as elevated levels of HNE have been associated with several human diseases, including chronic obstructive pulmonary disease (COPD), cystic fibrosis, acute lung injury (ALI), and acute respiratory distress syndrome (ARDS).[4,5] In addition, it has been reported that HNE can trigger tumor cell proliferation, and the use of HNE inhibitor can significantly augment the activity of antitumor agents.[6,7] The intensive efforts directed to the search for effective inhibitors for HNE over the past 2 decades have resulted in some limited successes: only three compounds (Elastatinal, AZD9668, and Bay719678) are currently in clinical trials, and a single drug called Sivelestat (Elaspol, ONO-5046) has been approved for clinical use.[8−10] The efficient method for measuring the activity of elastase with synthetic substrates may accelerate the development of drugs targeting HNE-related diseases.

Three major methods are currently available for assessing elastase's activity: monitoring elastase-mediated proteolysis of fibrinogen by high-performance liquid chromatography (HPLC) or liquid chromatography−mass spectrometry (LC−MS),[11,12] measuring UV−vis absorbance of proteolytic products (such as *p*-nitrophenol) using special colorimetric peptide substrates for elastase,[13−15] and tracking fluorescence changes of fluorescently modified peptide or protein substrates.[16] The HPLC method is time-consuming and not suitable for high-throughput experiments; the UV−vis and fluorometric methods are fast, sensitive, and compatible with high-throughput experiments, but both utilize specially produced, thus highly expensive, protein- or peptide-based substrates. Furthermore, most of such substrates are prone to degradation and thus require special storage. Since the substitution of nonpeptide substrates for protein- or polypeptide-based substrates offers an attractive alternative for assessing the activity of proteolytic enzymes,[17−21] we sought to create a non-peptide-based small-molecule substrate for HNE. Herein, we report the rational design of low-molecular weight non-peptide-based fluorescent probes as substrates for elastase. Hydrolysis of designed probes by HNE resulted in large enhancement of the fluorescence intensity. Accordingly, a "turn-on" fluorometric assay based on these novel probes was developed for rapid determination of HNE activity and the inhibitory kinetic study, demonstrating very low cost and high atom economy. High atom economy indicates the high conversion efficiency of a chemical process, which is the most widely used way to measure the "greenness" of a process or synthesis. In addition, the refined probe, compound **4**, was successfully applied to the detection of higher elastase activity in patients' serum compared to that in healthy controls.

Received: July 9, 2013
Accepted: October 28, 2013
Published: October 28, 2013

EXPERIMENTAL SECTION

Synthetic Chemistry of Compounds 1−4. Unless otherwise noted, all chemical reagents were commercially available and treated with standard methods before use. Silica gel column chromatography (CC): silica gel (200−300 mesh); Qingdao Makall Group Co., Ltd. (Qingdao, China). Solvents were dried in a routine way and redistilled. ^{1}H NMR and ^{13}C NMR spectra were recorded in $CDCl_3$ (or DMSO-d_6) on a Varian Mercury 600 or 400 spectrometer, and resonances (δ) are given in ppm relative to tetramethylsilane (TMS). ^{19}F NMR was recorded in CD_3OD on a Varian Mercury 400 spectrometer, and resonances (δ) are given in ppm relative to C_6F_6. The following abbreviations were used to designate chemical shift mutiplicities: s, singlet; d, doublet; t, triplet; m, multiplet; br, broad. High-resolution mass spectra (HRMS) were acquired in positive mode on a Waters MALDI SYNAPT G2 HDMS (MA, U.S.A.) or Agilent 6520 Accurate-Mass Q-TOF LC/MS (CA, U.S.A.).

7-Amino-4-trifluomethylcoumarin (M1) and 7-hydroxy-4-trifluoromethyl coumarin (M2) and were prepared by the reaction of ethyl 4,4,4-trifluoro-3-oxobutanoate with resorcinol or *m*-aminophenol according to the previous reports.[22,23] Then, the designed compounds **1**, **3**, and **4** were obtained by the nucleophilic attack of substituted anhydride toward M1, followed by subsequent elimination of HCl. Meanwhile, compound **2** was synthesized via the reaction between propionyl chloride and M2. The synthetic route is shown in Scheme 1, including the reactants and reaction conditions.

Scheme 1. Synthesis Route of Compounds 1−4[a]

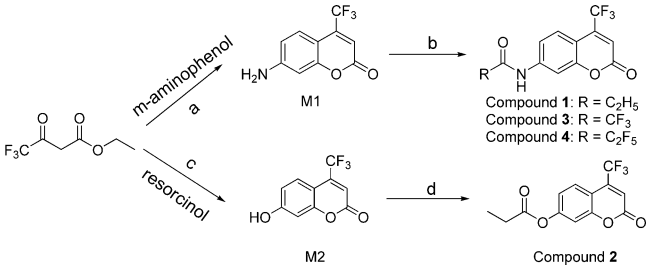

[a]Reagents and conditions: (a) $ZnCl_2$, EtOH, reflux; (b) RCOOCOR, pyridine, CH_2Cl_2, r.t.; (c) concd H_2SO_4, 1,4-dioxygen cyclohexane, reflux; (d) propionyl chloride, Et_3N, CH_2Cl_2, r.t.

Synthesis of Intermediate M1. Ethyl trifluoroacetoacetate (9.70 g, 55 mmol), 3-aminophenol (5.45 g, 50 mmol), and anhydrous $ZnCl_2$ (8.50 g, 62 mmol) were dissolved in EtOH (30 mL). The resulting mixture was refluxed for 8 h. When the reaction was completed, the mixture was cooled to the room temperature. The yellow solid was precipitated, filtered, and washed by cooled EtOH to obtain 7.05 g of 7-amino-4-trifluomethylcoumarin (M1). Yield: 56%. ^{1}H NMR (600 MHz, DMSO-d_6): δ 6.44−6.45 (m, 1H), 6.51−6.52 (m, 1H), 6.53 (s, 2H), 6.65−6.67 (m, 1H), 7.36−7.37 (m, 1H). EI−MS calcd for $[C_{10}H_6F_3NO_2]$: 229.16; found, 228.97.

Synthesis of Intermediate M2. Ethyl 4,4,4-trifluoro-3-oxobutanoate (1.84 g, 10 mmol) and resorcinol (1.1 g, 10 mmol) were dissolved in 1,4-dioxane (20 mL); 5 drops of concentrated sulfuric acid was added to the reaction mixture, and then it was refluxed for 5 h. After the reaction was completed, the mixture was poured into ice water (100 mL) and stirred, followed by precipitation and filtration. Then the crude product was recrystallized from the mixture of EtOH and H_2O to afford 1.2 g of pure M2 as a white solid. Yield: 52%. ^{1}H NMR (600 MHz, DMSO-d_6): δ 6.75 (s, 1H), 6.76 (s, 1H), 6.91 (d, J = 9.0 Hz, 1H), 7.56 (d, J = 7.2 Hz, 1H), 10.96 (s, 1H). HRMS (ESI$^+$) calcd for $[M + H^+]$: 231.0269; found, 231.0241.

Synthesis of Compounds **1**, **3**, *and* **4**. 7-Amino-4-trifluomethylcoumarin (229 mg, 1 mmol) and pyridine (158 mg, 2 mmol) were dissolved in anhydrous CH_2Cl_2 (10 mL). Then, the corresponding substituted anhydride or acyl chloride (1.2 mmol) was slowly added into the mixture under room temperature. The resulting reaction mixture was stirred and monitored by thin-layer chromatography (TLC). When the reaction was completed, the mixture was washed by water and saturated citric acid solution and extracted by CH_2Cl_2. The organic layer was dried by anhydrous Na_2SO_4, and the solvent was removed under the reduced pressure. The residue was purified by silica column chromatography to obtain the desired products **1**, **3**, and **4** as white solid.

Compound **1**. 178 mg. Yield: 63%. ^{1}H NMR (600 MHz, DMSO-d_6): δ 1.10 (t, J = 7.2 Hz, 3H), 2.4 (q, J = 7.8 Hz, 2H), 6.87 (s, 1H), 7.53−7.52 (m, 1H), 7.66 (d, J = 8.4 Hz, 1 Hz), 7.91 (s, 1H), 10.46 (s, 1H). ^{19}F NMR (376 MHz, CD_3OD): δ −65.02 ppm. EI−MS calcd for $[C_{13}H_{10}F_3NO_3]$: 285.22; found, 284.97. HRMS $[M - H]^-$: calcd, 284.0540; found, 284.0538.

Compound **3**. 195 mg. Yield: 60%. ^{1}H NMR (600 MHz, DMSO-d_6): δ 7.00 (s, 1H), 7.75 (s, 2H), 7.85 (s, 1H), 11.78 (s, 1H). ^{19}F NMR (376 MHz, CD_3OD): δ −76.99, −65.99 ppm. EI−MS calcd for $[C_{12}H_5F_6NO_3]$: 325.16; found, 324.95. HRMS $[M - H]^-$: calcd, 324.0100; found, 324.0095.

Compound **4**. 150 mg. Yield: 40%. ^{1}H NMR (600 MHz, DMSO-d_6): δ 7.03 (s, 1H), 7.79 (s, 2H), 7.88 (s, 1H), 11.82 (s, 1H). ^{19}F NMR (376 MHz, CD_3OD): δ −122.63, −83.31, −65.09 ppm. EI−MS calcd for $[C_{13}H_5F_8NO_3]$: 375.17; found, 374.94. HRMS $[M - H]^-$: calcd, 374.0069; found, 374.0079.

Synthesis of Compound **2**. M2 (0.46 g, 2 mmol) and Et_3N (0.61 g, 6 mmol) were dissolved in dichloromethane (DCM, 5 mL). Propionyl chloride (0.23 g, 2.4 mmol) in DCM (10 mL) was then slowly added, and the resulting mixture was stirred at room temperature for 2 h. After the reaction was completed as monitored by TLC, the solvent was removed under the reduced pressure. Then, the resulting crude product was washed by petroleum ether to obtain 0.38 g of pure compound **2** as a white solid. Yield: 67%. ^{1}H NMR (600 MHz, $CDCl_3$): δ 1.29 (t, J = 7.2 Hz, 3H), 2.65 (q, J = 7.2 Hz, 2H), 6.75 (s, 1H), 7.14 (d, J = 9 Hz, 1H), 7.21 (s, 1H), 7.71 (d, J = 9.0 Hz, 1H). ^{13}C NMR (150 MHz, $CDCl_3$): δ 171.76, 158.29, 154.84, 153.99, 140.92, 140.70, 25.97, 122.15, 120.33, 118.85, 115.10, 115.07, 110.93, 27.50, 8.64. HRMS (MALDI) calcd for $[M + H^+]$: 287.0531; found, 287.0516.

X-ray Diffraction Analysis of the Crystal Structure of 4. Compound **4** (20 mg) in CH_2Cl_2/petroleum ether (v/v = 1:2) solution was left to evaporate. Colorless single crystals suitable for X-ray diffraction were obtained. A suitable single crystal was selected and mounted in air onto thin glass fibers. Accurate unit cell parameters were determined by a least-squares fit of 2θ values, and intensity data were measured on a Bruker Smart CCD or Rigaku Raxis Rapid IP diffractometer with Mo Kα radiation (λ = 0.71073 Å) at room temperature. Lorentz polarization and absorption corrections were applied. The structures were solved by direct methods and refined with full-matrix least-squares technique using the SHELXS-97 and SHELXL-97 programs. All non-hydrogen atoms were refined with anisotropic thermal parameters.

dx.doi.org/10.1021/ac402097g | *Anal. Chem.* 2013, 85, 11304−11311

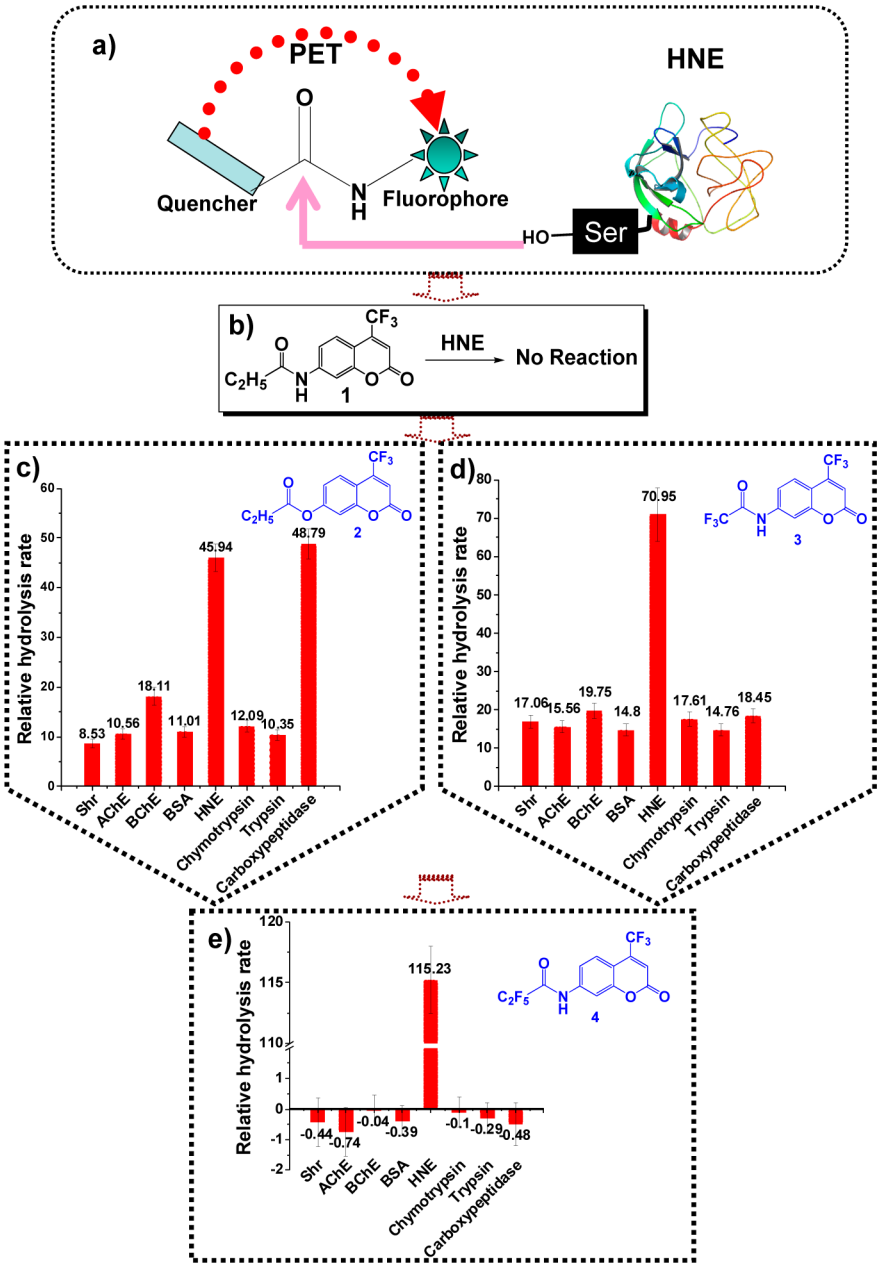

Figure 1. Design and optimization of the fluorescent probes for HNE. (a) The design strategy of the fluorescent probe based on the catalytic mechanism of HNE. (b) Chemical structure of compound **1** and HNE showed no activity toward compound **1**. (c–e) Chemical structures of compounds **2** (c), **3** (d), and **4** (e), and their stabilities and activities toward different hydrolases or proteins. Shr means the rate of spontaneous hydrolysis; AChE, BChE, and BSA are the abbreviations of acetylcholinesterase, butyrylcholinesterase, and bovine serum albumin, respectively. Their chemical structures were characterized by ^{1}H NMR, ^{13}C NMR, ^{19}F NMR, and HRMS (please see spectrum data in the Supporting Information).

Determination of Quantum Yield. The quantum yields of fluorescence were determined by comparison of the integrated area of the corrected emission spectrum of samples with a reference.[24] Specifically, using coumarin (Φ = 0.98, 0.1 M H_2SO_4) as reference, compounds **1**–**4**, 7-amino-4-trifluoromethyl coumarin (AFC), and 7-hydroxy-4-trifluoromethyl coumarin (HFC) were prepared in 0.1 M Tris–HCl (10 mM $CaCl_2$, pH 7.0) buffer and diluted to appropriate concentration to make their absorption less than 0.05. Then their UV–vis absorption spectrum was studied and the corresponding emission at relevant wavelength of excitation was measured as well. After correction of the refractive index of the different solvents determined by an Abbe's refractometer, the quantum yields were calculated with the expression in the following eq 1.

$$\phi_s = \frac{F_s A_c}{F_c A_s}\phi_c \quad (1)$$

UV–Vis Spectrophotometric Assay. Our assay on the in vitro elastase activity with or without inhibitors was measured by a modification of method previously reported in the literature using MeO-Suc-A-A-P-V-pNA as substrate.[25] Purified HNE obtained from Enzo life Science Company (Farmingdale, NY) was dissolved in 0.1 M Tris–HCl (10 mM $CaCl_2$, pH 7.0). MeO-Suc-A-A-P-V-pNA, Elastatinal, and Sivelestat purchased from Sigma-Aldrich company were prepared in water as stock

dx.doi.org/10.1021/ac402097g | *Anal. Chem.* 2013, 85, 11304–11311

solutions of 0.01 M, and aliquots of them were frozen at −20 °C. The reaction mixture in a total assay volume of 200 μL contained appropriate amounts of MeO-Suc-A-A-P-V-pNA, 0.1 M Tris−HCl buffer (10 mM $CaCl_2$, pH 7.0), inhibitor, and HNE. Enzymatic hydrolysis of MeO-Suc-A-A-P-V-pNA was monitored (SpectraMax M5, Molecular Devices) at 405 nm in the presence or absence of various concentrations of inhibitor at 30 °C, in 0.1 M Tris−HCl (10 mM $CaCl_2$, pH 7.0). Each experiment was repeated at least three times, and the values were averaged. On the basis of a plot of reciprocal enzymatic velocity (v) versus substrate concentration (S), the Michaelis constant (K_m) was calculated by referring to Lineweaver−Burk equation. The inhibition constant (K_i), the indication of an inhibitor's potency, was obtained from the Dixon plot of plotting $1/v$ against concentration of inhibitor at certain concentrations of substrate.[26] All the kinetic parameters were obtained by fitting the experimental data with Origin 8.0 software.

Fluorometric Assay. Fluorometric assay for elastase was performed as described in the following procedures by employing compounds **2**−**4** as substrates according to photoinduced electron-transfer (PET) mechanism. The weakly fluorescent substrate becomes highly fluorescent once the HNE cleaves the ester bond or amide bond, and the fluorescence enhancement is linearly correlated with the rate of hydrolysis at the early stage of the enzymatic reaction. Although the probes for elastase were designed based on the mechanism of PET, the inner filter effect as well as other possible factors that may affect fluorescent signal should be considered for accurate kinetic measurement. The dose-dependent fluorescence intensity of fluorescent chromophore (AFC or HFC) was measured in the absence and presence of various concentrations of substrate. Since compounds **3** and **4** shared the same fluorescent chromophore, here we only use **4** to study the possible interference effect for fluorometric assay. The concentration of each representative substrate (compounds **2**−**4**) was set to be 0.1, 0.2, 0.5, 1, 2, 5, 10 μM, which were utilized in the kinetic assays. The slope obtained from the fluorescence enhancement as the function of its concentration was converted as the correction factor of the fluorometric assay.

As to the kinetic assay, DMSO (as control) or various concentrations of inhibitor and appropriate amounts of desired compound as substrate were preincubated in 0.1 M Tris−HCl (containing 10 mM $CaCl_2$, pH 7.0) at 30 °C. Diluted HNE (50 μL) was then added to start the reaction, and the fluorescence signal was recorded at λ_{em} = 495 nm (λ_{exc} = 370 nm for AFC) and λ_{em} = 505 nm (λ_{exc} = 340 nm for HFC) by a microplate reader (SpectraMax M5, Molecular Devices) using a black microplate (96 wells), respectively. Each experiment was repeated at least three times, and the values were averaged. To obtain the initial reaction rate of each sample (μmol/min) we used the following formula for calculation:

$$v = -\ln\left(\frac{F_T - F_t}{F_T}\right)\frac{C}{t} \quad (2)$$

In the formula, F_t is the sample fluorescence intensity, F_T is the total fluorescence intensity when 100% substrate converted, C is the amount of substrate added to each vial, and t is incubation time in minutes. The Michaelis constant (K_m) was calculated by referring to the Lineweaver−Burk equation, and the inhibition constant (K_i) was obtained from the Dixon plot of plotting $1/v$ against concentration of inhibitor in the presence of a certain amount of substrate. All the kinetic parameters were also obtained by fitting the experimental data with Origin 8.0 software.

Human Serum Preparation and Activity Assay. Blood samples from patients or healthy people were collected in a separation gel−coagulant blood collection tube (Wuhan Zhiyuan Medical Technology, Co., Ltd. Wuhan), followed by clotting at 37 °C for 20 min of incubation. The resultant mixture was further centrifuged for 5 min, and the supernatant was isolated as serum and stored at 4 °C for later analysis.

As to the activity assay, the experimental procedures were described below. Before the assays start, compound **4** (0.2 mM) and 0.1 M Tris−HCl buffer (containing 10 mM $CaCl_2$, pH 7.0) were preincubated at 30 °C. The reaction was initiated by the addition of 50 μL of serum sample to the mixture of 10 μL of compound **4** (0.2 mM) and 140 μL Tris−HCl buffer (containing 10 mM $CaCl_2$, pH 7.0) in a black microplate (96 wells). The fluorescence signal of the reaction mixture was recorded at λ_{em} = 495 nm (λ_{ex} = 370 nm for AFC) by a microplate reader (SpectraMax M5, Molecular Devices). Each experiment was repeated at least three times, and the values were averaged.

RESULTS AND DISCUSSION

Probe Discovery. HNE uses its catalytic triad (made of the amino acid residues His-57, Asp-102, and Ser-195) to carry out the nucleophilic attack of an amide bond within a peptide substrate. On the basis of this mechanism, we directed our efforts to design small molecules that contain a central amide bond flanked by a pair of fluorophore and quencher (Figure 1a, PDB entry is 1HNE).[27] According to the PET mechanism, such intact molecules would exhibit a minimal level of fluorescence but, upon cleavage of the amide bond by HNE, should produce a high level of fluorescence.[28] We chose 7-amino-4-trifluoromethyl coumarin (AFC) as the fluorophore and the propionyl group as the quencher for the design of our first compound (compound **1**; Figure 1b). Upon extensive testing with various reaction conditions, we were disappointed to find that HNE did not show any hydrolytic activity toward **1**, although no detectable spontaneous hydrolysis was observed.

One possible explanation for the lack of detectable hydrolytic activity against **1** by HNE is that the amide bond of **1** is highly stabilized due to the delocalization of the nonpairing electrons into the benzene ring in AFC. To improve the hydrolytic activity of **1**, we tried two strategies. First, we substituted the amide bond with an ester bond (compound **2**, Figure 1c), which is known to be more prone to hydrolysis; second, we replaced the ethyl group with the trifluoromethyl group, which is a strong electron-withdrawing group, in an effort to enhance the nucleophilicity toward the carbonyl carbon (compound **3**, Figure 1d). As anticipated, both **2** and **3** were hydrolyzed by HNE (the reaction was monitored by the HPLC method; the detailed data are provided in Supporting Information Figure S1). However, both **2** and **3** displayed detectable rates of spontaneous hydrolysis under the reaction conditions, which are not suitable for in vitro and in vivo enzymatic assay. Interestingly, upon testing the hydrolysis of **2** and **3** under the same reaction conditions, we found that **3** displayed higher specificity for HNE (compare Figure 1, parts c and d) over other control proteins that usually exist in serum, including acetylcholinesterase (AChE), butyrylcholinesterase (BChE), chymotrypsin, trypsin, and carboxypeptidase, which represent

dx.doi.org/10.1021/ac402097g | Anal. Chem. 2013, 85, 11304−11311

alternative hydrolases, and bovine serum albumin (BSA) served as a nonhydrolase protein.

The above result revealed that the introduction of the trifluoromethyl group might enhance the specificity of the substrate for HNE over other hydrolytic enzymes. Meanwhile, the strong electron-withdrawing ability of the trifluoromethyl group appeared to reduce the stability of the amide bond, resulting in the increased spontaneous hydrolysis of **3**. On the basis of this observation, we synthesized compound **4**, 2,2,3,3,3-pentafluoro-*N*-(2-oxo-4-(trifluoromethyl)-2*H*-chromen-7-yl) propanamide, in which the trifluoromethyl group was replaced by a pentafluoroethyl group (Figure 1e) in an attempt to adjust the stability of the amide bond. The crystal structure of **4** (CCDC 918318) was confirmed by X-ray diffraction analyses (see Figure S2 in the Supporting Information). The hydrogen-bond network and stacking interactions within this compound are also provided (see Figure S3 in the Supporting Information). To our delight, there was no apparent spontaneous hydrolysis of **4** in the buffer system (100 mM Tris−HCl buffer contains 10 mM $CaCl_2$, pH 7.0) that was obtained by optimizing the buffer type, salt ions, additive agent, and pH value. It is also fairly stable in DMSO when stored at −20 and 4 °C for at least 3 months. More importantly, **4** showed further improved specificity for HNE since only HNE can hydrolyze **4** without any interfering hydrolysis of **4** by all the other tested hydrolases or proteins. In addition, the hydrolysis rate of **4** catalyzed by HNE is much higher than that of substrates **2** and **3** catalyzed by HNE. And those tested hydrolases or proteins displayed no obvious affect on the HNE-mediated fluorescence changes utilizing **4** as substrate (Table 1). Considering many other compounds or metal ions commonly found in biological fluids, we also investigated their possible interferences on the HNE-mediated fluorescence changes (Table 1). It revealed that most of the chosen analytes, including the metal ions and most of the amino acids, have no interference on the HNE activity even at very high concentration (100 μM), while only Glu showed up to about 10% reduction of HNE activity. Glucose and vitamin C both had no remarkable interference on HNE-mediated fluorescence assay at 100 μM.

Table 1. Interferences of the Representative Compounds Commonly Found in Biological Fluids on HNE-Mediated Fluorometric Assay, Using Compound 4 as Substrate

analyte	relative activity (%)	analyte	relative activity (%)
no analyte	100.00	$MnCl_2$ (100 μM)	103.57
AChE (1 μg/mL)	95.79	$ZnCl_2$ (100 μM)	108.51
BChE (1 μg/mL)	96.43	Trp (100 μM)	100.64
BSA (1 μg/mL)	95.55	Lys (100 μM)	109.97
chymotrypsin (1 μg/mL)	100.09	Ala (100 μM)	108.92
trypsin (1 μg/mL)	99.68	Phe (100 μM)	104.65
carboxypeptidase (1 μg/mL)	101.86	vitamin C (100 μM)	94.18
NaCl (100 μM)	98.35	Glu (100 μM)	86.85
$MgCl_2$ (100 μM)	105.45	His (100 μM)	97.98
KCl (100 μM)	112.44	Arg (100 μM)	102.92
LiCl (100 μM)	113.59	Cys (100 μM)	112.06
$FeCl_3$ (100 μM)	114.56	glucose (100 μM)	102.04
$CuSO_4$ (100 μM)	109.29	Met (100 μM)	94.47

We then examined HNE-mediated fluorescence changes of compound **4**. As shown in Figure 2a, **4** showed extremely weak background fluorescence, due to the mechanism of PET,[29,30] in the absence of HNE when excited at 370 nm. Upon the addition of HNE, hydrolysis occurred and green fluorescence that increased in intensity with respect to time was observed. In the presence of 0.02 unit/mL HNE, the maximum fluorescence intensity at 495 nm represented about a 20-fold increase over basal levels. The data indicated that **4** offered a robust fluorescence "turn-on" system for the detection of HNE activity. To check whether the robust fluorescence was caused by cleavage of the amide bond upon the addition of HNE, the reaction mixture was analyzed by HPLC. As indicated in Figure 2b, the peaks at 2.6 and 5.5 min were attributed to AFC and intact compound **4**, respectively. In the absence of HNE, only the peak of **4** was observed. In contrast, in the presence of HNE, the peak of AFC increased gradually with the reaction time, whereas the peak of **4** decreased accordingly. These results confirm that the amide bond of compound **4** has been cleaved by HNE.

Kinetic properties can aid in understanding the enzymatic mechanism of HNE. We therefore used compound **4** as substrate to measure the activity of HNE at 30 °C. To minimize the systematic experimental errors that may be caused by fluorescence quenching, including the possible inner filter effect, we measured the dose-dependent fluorescence intensity of fluorophore in the presence of various concentrations of substrates for correction (the data are offered in the Supporting Information, Table S1 and Figure S4). No significant fluorescence quenching effect was detected in our assay system, perhaps because (1) our probes were designed based on the PET mechanism instead of the fluorescence resonance energy transfer (FRET) that is usually associated with the inner filter effect; (2) a low range of substrate concentration (0−10 μM) was utilized in all the kinetic assays. Moreover, the plot of $1/v$ versus $1/S$ obeys the Lineweaver−Burk equation (Figure 3a and Supporting Information Figure S5). On the basis of the Lineweaver−Burk plots, the Michaelis constant (K_m) and the catalytic constant (k_{cat}) of HNE for **4** hydrolysis were determined to be 20.45 ± 1.85 μM and 21.84 ± 4.37 min^{-1}, respectively. Thus, the catalytic efficiency (k_{cat}/K_m) of HNE in processing **4** is about 1.07 $\mu M^{-1}\cdot min^{-1}$. In addition, we also investigated the k_{cat} and K_m using MeO-Suc-A-A-P-V-pNA, a previously reported peptide substrate for HNE, at the same temperature (see Figure 3b).[25,31] The k_{cat} for MeO-Suc-A-A-P-V-pNA hydrolysis by HNE was found to be 1200 ± 150 min^{-1}, ∼54-fold higher than that of **4**. However, the K_m of HNE for MeO-Suc-A-A-P-V-pNA (145 ± 12 μM) was ∼6-fold larger than that of **4**. Taken together, the overall catalytic efficiency of HNE against **4** is only ∼7-fold lower than that of MeO-Suc-A-A-P-V-pNA. This analysis indicates that **4** should be a suitable substrate for HNE. Furthermore, the limit of detection (LOD) for the method described herein was determined to be 68 ± 14 ng/mL based on five independent measurements.

It is well-known that the cost of the reagents is important for high-throughput drug discovery. Thus, we compared the cost between compound **4** and the peptide substrate commonly being used, MeO-Suc-A-A-P-V-pNA. It took just a few dollars (less than $10) for us to get 1 g of compound **4**, while MeO-Suc-A-A-P-V-pNA ($1755 per gram) is much more expensive

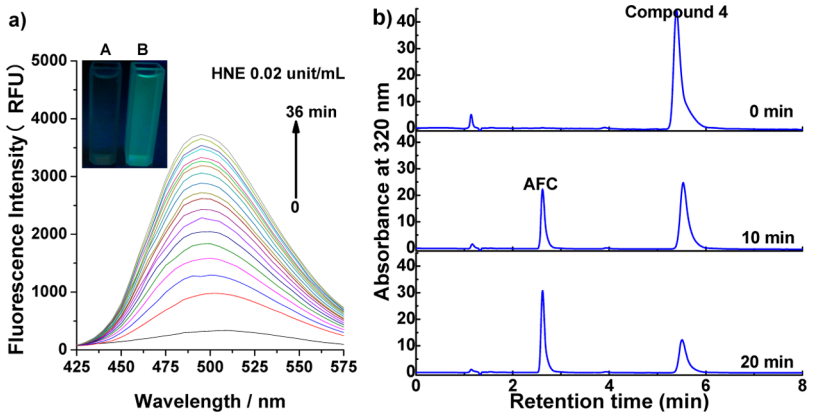

Figure 2. (a) Fluorescence spectra of the hydrolysis of compound **4** (10 μM) in the presence of HNE (0.02 unit/mL) incubated at 30 °C for different periods (100 mM Tris−HCl buffer contains 10 mM $CaCl_2$, pH = 7.0, λ_{ex} = 370 nm). The inset shows the photo of the corresponding reaction mixture in the absence (A) and presence (B) of 0.02 unit/mL HNE after incubation for 10 min under UV light at 365 nm. (b) Time-dependent HPLC analysis of the hydrolysis of compound **4** (100 μM) in the presence of HNE (0.1 unit/mL). AFC represents 7-amino-4-trifluoromethyl coumarin. The negative peaks are attributed to the solvent of DMSO.

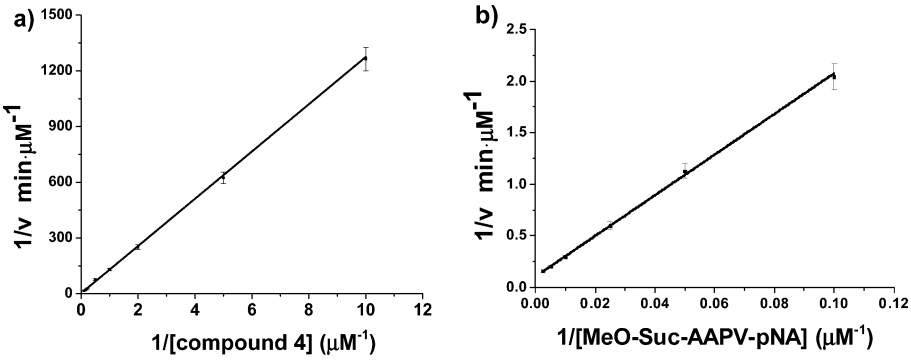

Figure 3. (a) Lineweaver−Burk plot of compound **4** hydrolysis catalyzed by HNE with the fluorometric method. (b) The Lineweaver−Burk plot of MeO-Suc-A-A-P-V-pNA hydrolysis catalyzed by HNE with the UV−vis method.

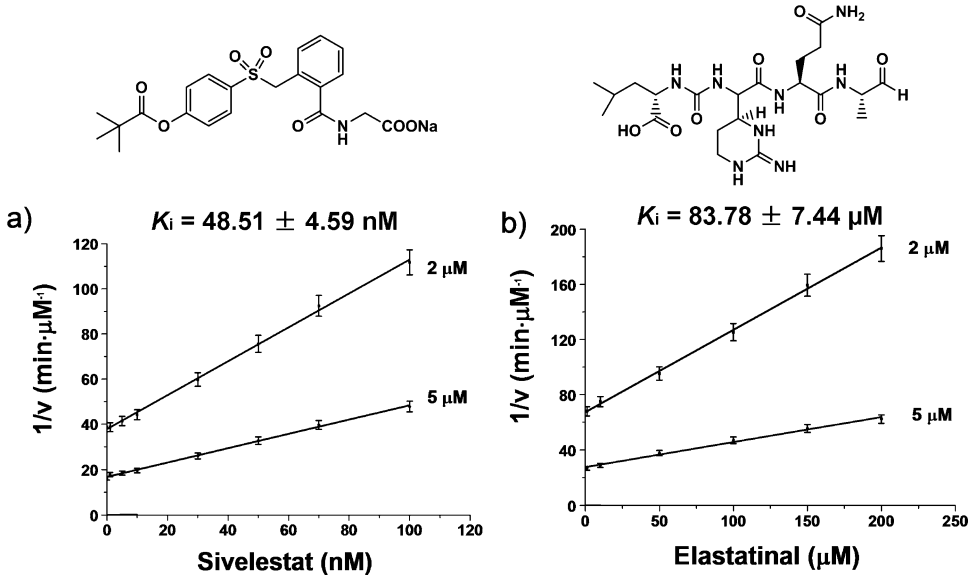

Figure 4. Dixon plots of inhibitory kinetics of Sivelestat (a) and Elastatinal (b) with compound **4** as the substrate.

according to the report on the Web site of Sigma-Aldrich company.

Inhibitory Kinetics. Next, we carried out the HNE inhibition study using compound **4** as a reporter. Two well-known reversible HNE inhibitors, Sivelestat and Elastatinal, were selected as the references. As a control, we also performed a comparative study using MeO-Suc-A-A-P-V-pNA as the substrate.[32] The time course of inhibitory kinetics of HNE clearly demonstrated that Sivelestat is a classical reversible inhibitor without any slow binding phenomenon (see Figure S6

dx.doi.org/10.1021/ac402097g | *Anal. Chem.* 2013, 85, 11304−11311

in the Supporting Information). As shown in Figure 4, parts a and Figure b, both Sivelestat and Elastatinal indeed displayed a linear relationship of reciprocal rate versus inhibitor concentration like other classical reversible inhibitors do, similar to that of MeO-Suc-A-A-P-V-pNA as substrate. Using **4** as the substrate, K_i values for Sivelestat and Elastatinal are 48.51 nM and 83.78 μM, respectively. Very similar K_i values, 48.14 nM and 84.21 μM, were obtained with MeO-Suc-A-A-P-V-pNA as the substrate (see Figure S7 in the Supporting Information). Therefore, compound **4** can be used as a reliable fluorogenic reagent for screening and characterizing HNE inhibitors under moderate conditions.

Primary Application in Clinical Diagnosis. Extensive work has shown that the level of HNE can be a predicting factor for monitoring the development of some common human diseases such as COPD, ALI/ARDS, pulmonary dysfunction, and infertility.[11,33−35] The enzyme-linked immunosorbent assay (ELISA) method has been commonly used for quantitative determination of human elastase in diagnostic procedures, but it is time-consuming and costly.[36,37] Furthermore, the results of the ELISA method always reflect the concentration of total elastase rather than the concentration of only the active form of elastase. Here, we sought to evaluate the utility of compound **4** in detecting elastase activity in crude serum of some COPD patients. After collection of blood from patients or healthy people, the serum samples were prepared and their elastase activities were further assessed according to the methods described before. As depicted in Figure 5, the

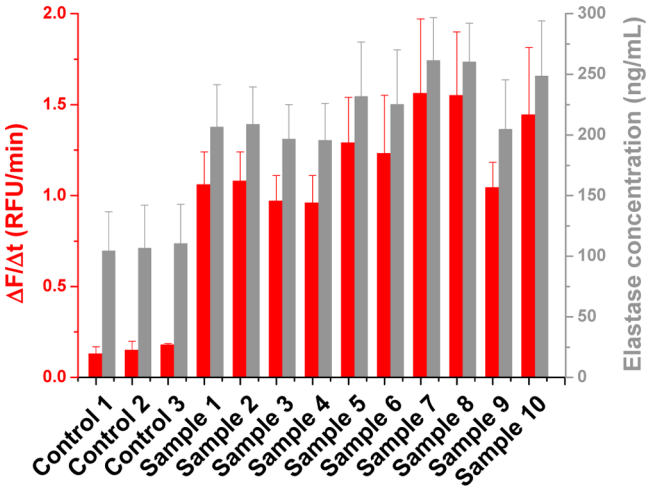

Figure 5. Relative hydrolysis rates ($\Delta F/\Delta t$, red color) of compound **4** in the serum of the healthy controls (controls 1−3) and COPD patients (samples 1−10) and the absolute concentrations (dark gray color) of active elastase in the serum of corresponding healthy persons and patients.

relative hydrolytic rate ($\Delta F/\Delta t$) of compound **4** in the serum of 10 COPD patients is about 7−10-fold higher than that in three healthy controls. In addition, we calculated the absolute concentrations of active elastase in the serum of these patients and healthy controls. The active elastase level in healthy people was found to be 105 ± 2.8 ng/mL, whereas the corresponding level in 10 COPD patients ranged from 195 ± 31 to 261 ± 35 ng/mL based on the standard addition method,[38] about 2-fold higher than that of healthy controls. Compared to the ELISA methods which usually cost 3 h or more, the fluorometric assay described herein only takes about 10 min for detecting elastase activity, without utilizing expensive antibody reagents. These results indicate that compound **4** has potential utility for clinical diagnosis for elastase-related diseases.

CONCLUSION

In conclusion, we have successfully designed a small-molecule compound, 2,2,3,3,3-pentafluoro-*N*-(2-oxo-4-(trifluoromethyl)-2*H*-chromen-7-yl)propanamide, that can be used as a fluorogenic substrate for elastase, a protease that is implicated in several human diseases. To our knowledge, this is the first ever non-peptide-based fluorogenic substrate for elastase. This small organic molecule can easily be synthesized and does not require special storage. More importantly, it can be used to set up an efficient and cost-effective fluorescent assay for tracking the enzymatic activity of HNE. The assay features very low background noise, high specificity, and ideal detection limit (LOD = 68 ± 14 ng/mL) and is compatible with high-throughput experiments. Therefore, this assay should be useful for future high-throughput campaigns in search of HNE inhibitors. We have also demonstrated that this small-molecule probe can be directly used to detect the elevated elastase activity in the serum of COPD patients, pointing to its potential to be used in clinical diagnosis of elastase-related diseases.

ASSOCIATED CONTENT

Supporting Information

Additional information as noted in text. This material is available free of charge via the Internet at http://pubs.acs.org.

AUTHOR INFORMATION

Corresponding Authors

*E-mail: tomyang@mail.ccnu.edu.cn. Phone: 86-27-67867706. Fax: 86-27-67867141 (W.-C.Y.).
*E-mail: gfyang@mail.ccnu.edu.cn. Phone: 86-27-67867800. Fax: 86-27-67867141 (G.-F.Y.).

Author Contributions

§Q.S. and J.L. contributed equally to this work.

Notes

The authors declare no competing financial interest.

ACKNOWLEDGMENTS

This work was funded by the National Natural Science Foundation of China (NSFC; Nos. 20925206, 21102052, and 21372094) and the National Basic Research Program of China (No. 2010CB126103).

REFERENCES

(1) Kinoshita, M.; Ono, S.; Mochizuki, H. *Eur. Surg. Res.* **2000**, *32*, 337−346.
(2) Kawabata, K.; Hagio, T.; Matsuoka, S. *Eur. J. Pharmacol.* **2002**, *451*, 1−10.
(3) Pham, C. T. *Int. J. Biochem. Cell Biol.* **2008**, *40*, 1317−1333.
(4) Bousquet, J.; Khaltaev, N. G.; Cruz, A. A. *Global surveillance, prevention and control of chronic respiratory diseases: A comprehensive approach*; WHO Press: Geneva, Switzerland, 2007.
(5) *Chronic respiratory diseases*. http://www.who.int/respiratory/en/. World Health Organization, 2012.
(6) Nawa, M.; Osada, S.; Morimitsu, K.; Nonaka, K.; Futamura, M.; Kawaguchi, Y.; Yoshida, K. *Anticancer Res.* **2012**, *32*, 13−19.
(7) Moroy, G.; Alix, A. J.; Sapi, J.; Hornebeck, W.; Bourguet, E. *Anti-Cancer Agents Med. Chem.* **2012**, *12*, 565−579.
(8) Schepetkin, I. A.; Khlebnikov, A. I.; Quinn, M. T. *J. Med. Chem.* **2007**, *50*, 4928−4938.

(9) Imaki, K.; Okada, T.; Nakayama, Y.; Nagao, Y.; Kobayashi, K.; Sakai, Y.; Mohri, T.; Amino, T.; Nakai, H.; Kawamura, M. *Bioorg. Med. Chem.* **1996**, *4*, 2115−2134.
(10) Mittendorf, E. A.; Alatrash, G.; Qiao, N.; Wu, Y.; Sukhumalchandra, P.; St. John, L. S.; Philips, A. V.; Xiao, H.; Zhang, M.; Ruisaard, K.; Clise-Dwyer, K.; Lu, S.; Molldrem, J. J. *Cancer Res.* **2012**, *72*, 3153−3162.
(11) Weitz, J. I.; Landman, S. L.; Crowley, K. A.; Birken, S.; Morgan, F. J. *J. Clin. Invest.* **1986**, *78*, 155−162.
(12) Wang, Y.; Zagorevski, D. V.; Stenken, J. A. *Anal. Chem.* **2008**, *80*, 2050−2057.
(13) Bieth, J.; Spiess, B.; Wermuth, C. G. *Biochem. Med.* **1974**, *11*, 350−357.
(14) Castillo, M. J.; Nakajima, K.; Zimmerman, M.; Powers, J. C. *Anal. Biochem.* **1979**, *99*, 53−64.
(15) Rao, S. K.; Mathrubutham, M.; Karteron, A.; Sorensen, K.; Cohen, J. R. *Anal. Biochem.* **1997**, *250*, 222−227.
(16) Palmier, M. O.; Fulcher, Y. G.; Van Doren, S. R. *Anal. Biochem.* **2011**, *408*, 172−174.
(17) Masler, E. P. *J. Helminthol.* **2002**, *76*, 45−52.
(18) Ruan, B. H.; Cole, D. C.; Wu, P.; Quazi, A.; Page, K.; Wright, J. F.; Huang, N.; Stock, J. R.; Nocka, K.; Aulabaugh, A.; Krykbaev, R.; Fitz, L. J.; Wolfman, N. M.; Fleming, M. L. *Anal. Biochem.* **2010**, *399*, 284−292.
(19) Fan, Y.; Hense, M.; Ludewig, R.; Weisgerber, C.; Scriba, G. K. E. *J. Pharm. Biomed. Anal.* **2011**, *54*, 772−778.
(20) Noble, J. E.; Ganju, P.; Cass, A. E. *Anal. Chem.* **2003**, *75*, 2042−2047.
(21) Hitomi, Y.; Takeyasu, T.; Funabiki, T.; Kodera, M. *Anal. Chem.* **2011**, *83*, 9213−9216.
(22) Bissell, E. R.; Mitchell, A. R.; Smith, R. E. *J. Org. Chem.* **1980**, *45*, 2283−2287.
(23) Zhang, C. S.; Chen, Y.; Xu, X. Q.; Liu, X.; Yu, M. Q.; Liu, B. F.; Liu, Z. Q. Chinese Patent CN102267966, 2011.
(24) Qian, F.; Zhang, C.; Zhang, Y.; He, W.; Gao, X.; Hu, P.; Guo, Z. *J. Am. Chem. Soc.* **2009**, *131*, 1460−1468.
(25) Nakajima, K.; Powers, J. C.; Ashe, B. M.; Zimmerman, M. *J. Biol. Chem.* **1979**, *254*, 4027−4032.
(26) Dixon, M. *Biochem. J.* **1972**, *129*, 197−202.
(27) Navia, M. A.; McKeever, B. M.; Springer, J. P.; Lin, T. Y.; Williams, H. R.; Fluder, E. M.; Dorn, C. P.; Hoogsteen, K. *Proc. Natl. Acad. Sci. U.S.A.* **1989**, *86*, 7−11.
(28) Wysocka, M.; Lesner, A.; Gruba, N.; Korkmaz, B.; Gauthier, F.; Kitamatsu, M.; Legowska, A.; Rolka, K. *Anal. Chem.* **2012**, *84*, 7241−7248.
(29) Liu, Z.; Zhang, C.; Li, Y.; Wu, Z.; Qian, F.; Yang, X.; He, W.; Gao, X.; Guo, Z. *Org. Lett.* **2009**, *11*, 795−798.
(30) Xue, L.; Liu, Q.; Jiang, H. *Org. Lett.* **2009**, *11*, 3454−3457.
(31) Yasutake, A.; Powers, J. C. *Biochemistry* **1981**, *20*, 3675−3679.
(32) Groth, I.; Alban, S. *Planta Med.* **2008**, *74*, 852−858.
(33) Hautamaki, R. D.; Kobayashi, D. K.; Senior, R. M.; Shapiro, S. D. *Science* **1997**, *277*, 2002−2004.
(34) Zorn, B.; Virant-Klun, I.; Meden-Vrtovec, H. *Hum. Reprod.* **2000**, *15*, 1978−1984.
(35) Kodama, T.; Yukioka, H.; Kato, T.; Kato, N.; Hato, F.; Kitagawa, S. *Intern. Med. (Tokyo, Jpn.)* **2007**, *46*, 699−704.
(36) Papadaki, H. A.; Horwitz, M.; Coulocheri, S. A.; Person, R. A.; Benson, K. F.; Eliopoulos, G. D. *Blood* **2003**, *101*, 2898−2899.
(37) Wang, Z. X.; Chen, F.; Zhai, R. H.; Zhang, L. S.; Su, L.; Lin, X. H.; Thompson, T.; Christiani, D. C. *PLoS ONE* **2009**, *4* (2), e4380.
(38) Ros-Lis, J. V.; Garcia, B.; Jimenez, D.; Martinez-Manez, R.; Sancenon, F.; Soto, J.; Gonzalvo, F.; Valldecabres, M. C. *J. Am. Chem. Soc.* **2004**, *126*, 4064−4065.